analytical chemistry

Article

pubs.acs.org/ac

Versatile Tool for the Analysis of Metal–Protein Interactions Reveals the Promiscuity of Metallodrug–Protein Interactions

Ronald F. S. Lee, Laure Menin, Luc Patiny, Daniel Ortiz, and Paul J. Dyson*

Institute of Chemical Sciences and Engineering, Swiss Federal Institute of Technology Lausanne (EPFL), Lausanne CH-1015, Switzerland

Supporting Information

ABSTRACT: Metallodrug–protein interactions contribute to their therapeutic effect (even when DNA is the dominant target), side-effects and are implicit in drug resistance. Here, we provide mass spectrometric-based evidence to show that metallodrug interactions with proteins are considerably more complex than current literature would suggest. Using native-like incubation and electrospray conditions together with an automated tool we designed for exhaustive mass spectra matching, the promiscuity of binding of cisplatin to ubiquitin is revealed, with 14 different binding sites observed. There is a binding preference to negatively charged sites on the protein, consistent with the cationic nature of the cisplatin adduct following aquation. These results have implications in metallodrug development and beyond to the toxicological effects of metal ions more generally.

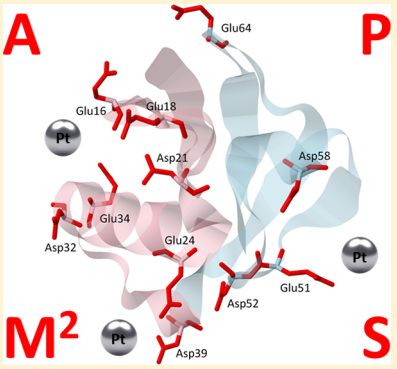

The interaction of metal ions with proteins is important as many endogenous proteins utilize metals for stabilization or activity.[1] Metal complexes are also used therapeutically for the diagnosis or treatment or various diseases,[2] and certain metal ions are also implicated in toxicity and diseases.[3] Many techniques have been used to study metal–protein interactions[4−6] and mass spectrometry (MS) has been particularly valuable,[7−17] leading to the field of metallomics.[18] Notably, the application of top-down tandem MS, where whole proteins are directly sprayed into the mass spectrometer and then fragmented (MS/MS),[19,20] has been extremely useful in identifying binding sites of metallodrugs. Various metal–protein interactions have been probed by the application of top-down MS.[8,10,11,14−16,21,22] However, a significant challenge of this approach is to interpret the complicated mass spectra generated where typically thousands of peaks are present, and manual identification is extremely difficult (due to the vast number of complex and overlapping isotopic patterns observed from metal species adducted to peptide fragments), prone to error, and often only the most intense peaks are assigned. In this context, previous studies do not use internal fragment ions generated by CID to assign metalation sites.

To overcome this limitation, we developed an automated tool, termed Analysis of Protein Modifications from Mass Spectra (Apm^{2}s), a free and versatile web-based tool based on chemcalc (http://ms.cheminfo.org/apm2s/index.html).[23] This tool calculates all possible theoretical mass spectra of a given protein/peptide sequence with any user defined modifications (e.g., post translational modifications, ligands, metal ions) and matches each individual isotopic peak to experimental mass spectra to generate a list of matches with similarity scores[24] (matching algorithm described in further detail in the SI). Using this tool to decipher the binding sites of cisplatin incubated with ubiquitin, chosen as an extensively studied system, we discovered that far more potential binding sites exist than current MS studies have identified.

Clinically, cisplatin is one of the most widely used cancer chemotherapy agents,[25,26] and MS-based studies of its binding to the 8.5 kDa protein ubiquitin (Ubi) have been performed previously by MS.[21,27,28] The binding of cisplatin to either unmodified and oxidized ubiquitin was compared revealing that oxidation of the Met1 residue reduced cisplatin binding, indicating Met1 is a potentially important binding site.[27] This binding site was subsequently confirmed in a top-down study where platinated fragments containing Met1 were identified when the cisplatin-ubiquitin adduct was fragmented by either collisional induced dissociation (CID) and infrared multiphoton dissociation (IRMPD).[21] A bottom-up study of the same system has also been performed identifying up to four different binding sites, Met1, Thr12, Thr14, and Asp32.[28] These previous studies provided us a basis for comparing our own results using the automated tool.

EXPERIMENTAL SECTION

Materials. Ubiquitin from bovine erythrocytes and myoglobin from equine skeletal muscle was purchased from Sigma-Aldrich (Product number U6253 and M0630 respectively) and cisplatin was purchased from Tokyo Chemical Industries. MS grade LysylC and GluC endoproteinase were

Received: June 8, 2017
Accepted: October 20, 2017
Published: October 20, 2017

DOI: 10.1021/acs.analchem.7b02211
Anal. Chem. 2017, 89, 11985−11989

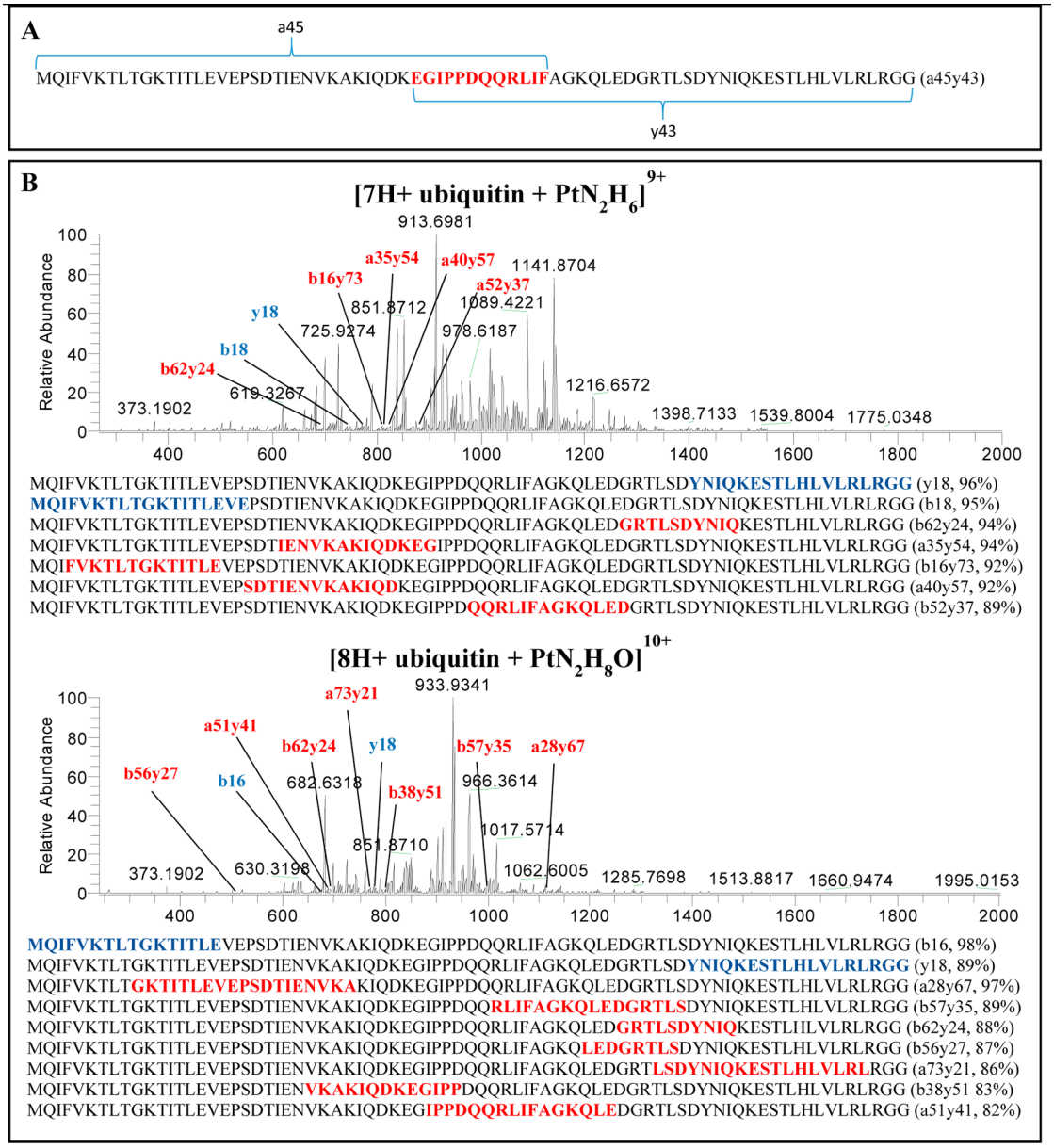

Figure 1. Top-down MS/MS from the CID fragmentation of the $[7H + Ubi + PtN_2H_6]^{9+}$ and $[8H + Ubi + PtN_2H_8O]^{10+}$ ions. (A) Explanation of the internal fragment nomenclature of the Apm[2]s tool. Internal fragment named (N-terminal fragment, C-terminal fragment) and corresponds to the regions which overlap between the N and C terminal fragments. (B) MS/MS spectra with detected metalated fragments labeled (terminal fragments in blue and internal fragments in red). Location of metalated fragments in full length ubiquitin is shown below each spectra and similarly color coded with adduct type and calculated similarity score in brackets (only metalated fragments with <20 amino acid residues are shown for clarity).

purchased from Thermo Fisher Scientific, U.S.A. RAPTA-C was synthesized from a literature procedure.[29]

Sample Preparation. Ubiquitin (100 μM) was incubated with cisplatin in 1:1, 1:5 and 1:30 protein:drug ratios at 37 °C for 0.5 to 18 h. Myoglobin (10 μM) was incubated with RAPTA-C in 1:3 ratio at 37 °C for 24 h. All incubations were performed in sterile MilliQ water. Excess drug was removed with three rounds of centrifugation using 3 kDa-cutoff Amicon Ultra centrifugal filters according to manufacturer's instructions. Incubated proteins were snap frozen in liquid N_2 and stored at −20 °C prior to MS/MS analysis. For bottom-up sample preparation, metallodrug−protein incubations were digested with MS grade LysylC according to manufacturer's instructions. In brief, incubation of ubiquitin with each enzyme was performed at a ratio of 1:50 in a 5 mM ammonium carbonate pH 8 buffer, for 8 h at 37 °C.

Mass Spectrometry Analysis. CID fragmentation studies were performed on an ETD enabled hybrid linear ion trap (LTQ) Orbitrap Elite mass spectrometer (Thermo Scientific, Bremen, Germany) coupled to a Triversa Nanomate (Advion) chip-based electrospray system. For top-down experiments, samples were diluted in water and directly infused. For bottom-up samples, dilutions were performed in CH_3CN/H_2O/HCOOH (50:49.9:0.1) before infusion. Spray voltage used was 1.6 kV and the automatic gain control (AGC) target was set to 1×10^6 for full scans in the Orbitrap mass analyzer. Precursor ions for MS/MS were detected in the Orbitrap at a resolving power of 30000 (at 400 m/z) with an isolation width of 8, and product ions were transferred to the FT-MS operated

DOI: 10.1021/acs.analchem.7b02211
Anal. Chem. 2017, 89, 11985−11989

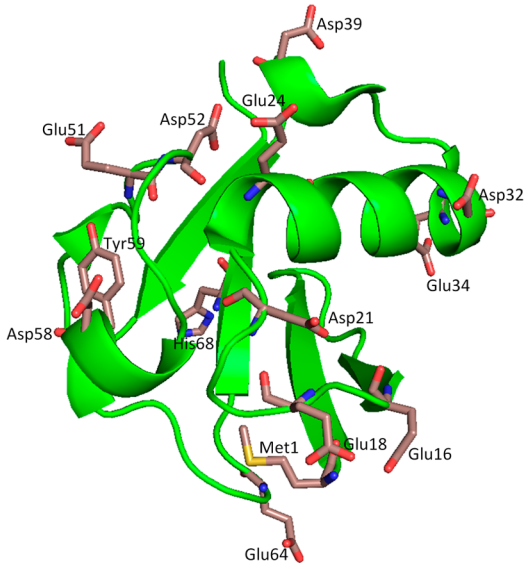

MQIFVKTLTGKTITLEVEPSDTIENVKAKIQDKEGIPPDQQRLIFAGKQLEDGRTLSDYNIQKESTLHLVLRLRGG

Figure 2. Most likely binding sites of the platinum(II) ion on bovine ubiquitin. Crystal structure of bovine ubiquitin in green with likely binding residues represented in stick figures (top) and full amino acid sequence of bovine ubiquitin with predicted binding sites highlighted in red (bottom).

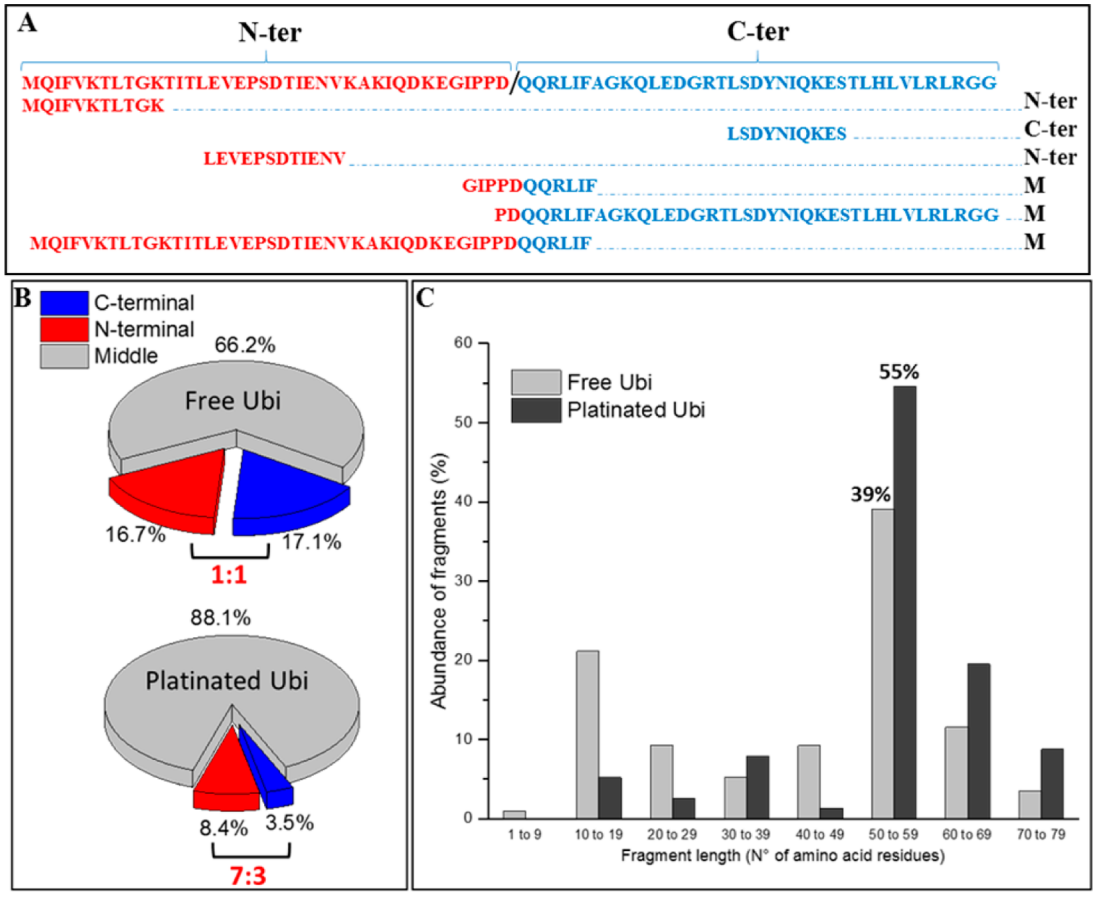

Figure 3. (A) Classification of N-ter, C-ter, and M fragments. Full sequence of ubiquitin with classification on top with examples in each row. N-terminal fragments from residue 1−39 named N-ter (in red), fragments from residues 40−76 named C-ter (in blue), and all other fragments named M (containing both blue and red). (B) Percentage abundance of N-ter, C-ter, and M fragment ions from CID fragmentation of free ubiquitin (top) and platinated ubiquitin at a 1:1 protein: drug ratio (bottom) following 18 h incubation at 37 °C. (C) Percentage abundance of CID fragments classified into different amino acid lengths from CID fragmentation of free ubiquitin and platinated ubiquitin (similar incubation conditions as above). Parents ions $[9H+\ Ubi]^{9+}$, $[10H+\ Ubi]^{10+}$, $[7H+\ Ubi + PtN_2H_6]^{9+}$, $[8H+\ Ubi + PtN_2H_8O]^{10+}$ were used for the fragmentation study.

DOI: 10.1021/acs.analchem.7b02211
Anal. Chem. 2017, 89, 11985−11989

with an AGC of 5×10^4 over a m/z range of 200−3000. For CID and HCD fragmentation, normalized collision energies of 20−35% and 23% respectively were used. A total of 100 scans and 10 μscans were acquired in reduced profile mode and averaged for each fragmentation spectra. Spectra was exported using Thermo Xcalibur software as .txt files and imported directly into the Apm^{2}s tool for further downstream processing.

Data Processing and Analysis. Details available in Supporting Information (SI).

RESULTS AND DISCUSSION

In our study cisplatin was incubated with ubiquitin in pure water (pH 6.1), which retains the protein in a native-like state (Figure S5, SI).[28,30] Top-down MS/MS via collision induced dissociation (CID) was applied on ubiquitin incubated with cisplatin for 18 h at 37 °C. The $[7H + Ubi + PtN_2H_6]^{9+}$ and $[8H + Ubi + PtN_2H_6]^{10+}$ precursor ions were selected for fragmentation and a list of more than 200 metalated fragment ions were assigned with similarity scores above 80% from the tool analysis (Tables S3 and S4, SI). The Apm^{2}s tool uses protein/peptide sequences with user defined modifications incorporating any element in the periodic table (for a detailed description see the SI). For top-down MS specifically, the tool identifies a, b, c, x, y, and z fragment ions and, importantly, also identifies internal fragments which, to the best of our knowledge, other automated matching solutions do not allow.

Surprisingly, the metalated ions found span the full sequence of ubiquitin (Figure 1B) and, consequently, we conducted a closer analysis to identify the most likely binding residues. Considering the amino acid side chains containing lone pairs which can coordinate to the metal center (side chains with carboxylic acid, phenol, amino, or sulfur groups) and the incubation pH of 6.1 (causing protonation of amine side chains but leaving carboxylic acid side chains deprotonated), a total of 14 possible platinum coordination sites were identified (Figure 2). From the crystal structure representation (Figure 2), most amino acid side chains are pointing outward toward solvent allowing access for metal binding. From the CID fragments obtained, platinum potentially binds to all 14 sites. This finding is also supported that up to seven platinated adducts are detected after 18 h incubation of ubiquitin with a 30-fold excess of cisplatin (Figure S4, SI), demonstrating the presence of multiple binding sites of platinum on ubiquitin.

As mentioned above, previous studies had identified only one platinum binding site (Met1) from top-down MS and up to four (Met1, Thr12, Thr14, and Asp32) via bottom-up approaches,[21,27,28] the larger number in the latter possibly due to detachment and rebinding reactions taking place during the digestion process. The identification of up to 14 binding sites via top-down MS highlights the importance of automated identification of all possible metalated ion species, including metalated internal fragments which are otherwise obscured. Moreover, these findings highlight the complexity of metallodrug binding to proteins which are probably mediated by multidentate interactions (see SI). The results from top-down studies were confirmed by bottom-up experiments where metalated digest fragments spanning the full sequence of ubiquitin were observed (Figure S6, SI), indicative of the same 14 different binding sites. Analysis of the bottom-up data was similarly performed by the Apm^{2}s tool, which is amenable to matching of enzymatically digested protein fragments.

The abundance of metalated/unmetalated CID fragments was analyzed to establish whether there is any preference of cisplatin binding along the ubiquitin sequence. Starting from the N-terminus, fragment ions from residues 1−39 were named N-ter, and those including residues 40−76 were named C-ter, with all other fragment ions named M for middle (nomenclature detailed in Figure 3A). Upon platination, there is a clear shift from a near 1:1 ratio of N-ter: C-ter fragments in free ubiquitin to a 7:3 ratio of N-ter:C-ter in platinum bound ubiquitin, showing a preference of formation of N-ter metalation (Figure 3, B). This difference indicates that platination occurs preferentially on the N-terminal half of ubiquitin, which may be rationalized from isoelectric point (PI) calculations of both halves of the protein. The N-terminal region of ubiquitin, which contains more acidic side chain amino acids, has a PI of 4.62, giving it a more negative polarity than the C-terminal region with a PI of 9.34 (Figure 4).

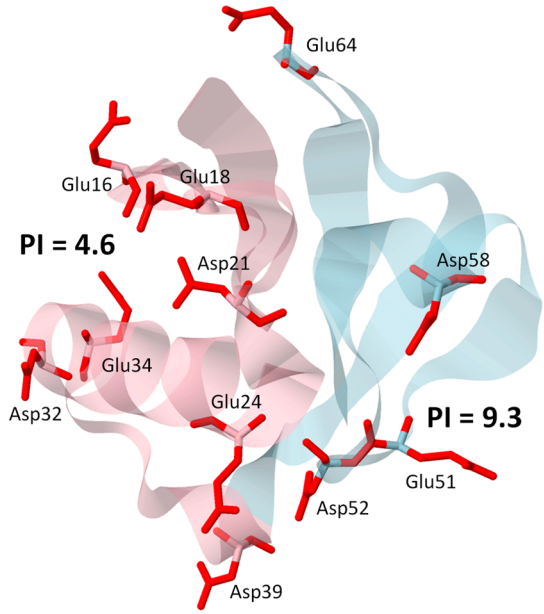

Figure 4. Ribbon crystal structure of bovine ubiquitin indicating the N-ter and C-ter portions of the protein (colored in translucent red and light blue, respectively) with isoelectric point values labeled. Acidic amino acid residues (Glu and Arg) are labeled in red.

Considering that cisplatin is a prodrug and that aquation involves formation of the active cationic intermediates (Figure 5)[31] attraction to the negatively charged region of ubiquitin would be expected, leading to the observed binding preference.

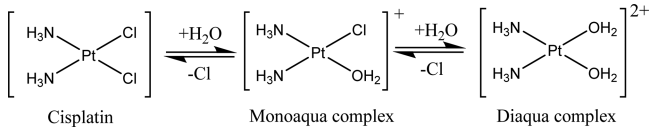

Figure 5. Aquation reactions of cisplatin.

Upon platinum binding, there is an increase in the proportion of M fragments as a fraction of total fragments, from 66% in free ubiquitin to 88% in metalated ubiquitin (Figure 3B). This shift in distribution is also accompanied with an increase in the average length of fragment ions obtained upon metal binding (Figure 3C). From the availability of up to 14 different platinum binding sites on ubiquitin and the formation of ions containing up to seven platinums in the

DOI: 10.1021/acs.analchem.7b02211
Anal. Chem. 2017, 89, 11985−11989

presence of 30-fold excess of drug (Figure S4, SI), presumably binding of cisplatin to ubiquitin occurs mostly in a bi-, tri-, and tetra-dentate manner. Such binding potentially connects peptide fragments, thus during CID fragmentation of the peptide backbone these connected fragments stay intact leading to the observed increased proportion of M fragments and higher average lengths of metalated fragments. Alternatively part of the CID energy could be spent on dissociation of ligands coordinated to the platinum center, leaving less energy available for fragmentation of the protein.

As validation of the Apm^{2}s tool on a different metal-protein system, we used the tool to study the interaction of a ruthenium(II) drug, RAPTA-C, on the 17 kDa protein myoglobin (data provided in the SI). The tool is able to detect ruthenium adducts and loss of heme on myoglobin highlighting its applicability to larger proteins and different metals. Studies on more complex systems (larger proteins, different fragmentation methods, and various protein modifications) will be carried out in the future to improve the tools performance.

CONCLUSIONS

This study highlights the importance of matching all MS/MS fragment peaks including internal fragments when performing top-down MS experiments to study metallodrug−protein interactions. Exhaustive matching using the Apm^{2}s tool disclosed here provides an abundance of data which can give valuable insight into metal-protein binding. Specifically, we have shown that cisplatin binding to ubiquitin appears to be far more complex than currently thought, with evidence to support up to 14 different binding sites, with a preference for the negatively charged, accessible regions of the protein. These findings have implications in design of targeted metallodrugs where the complexity and promiscuity of metallodrug binding to proteins necessitates careful consideration of the metal center and associated ligands to achieve the desired selectivity. Besides our application, the Apm^{2}s tool could also be used to study metal toxins and should greatly facilitate metallomics studies, which are currently attracting considerable attention in both the cause and prevention of various diseases. For the broader MS community, the analysis tool can be applied to studies involving proteins modified with virtually any element in the periodic table and would greatly facilitate data analysis for such applications.

ASSOCIATED CONTENT

Supporting Information

The Supporting Information is available free of charge on the ACS Publications website at DOI: 10.1021/acs.analchem.7b02211.

Additional data and figures described in the manuscript. Information regarding the Apm^{2}s tool which includes the matching algorithm, input parameters and data interpretation restrictions applied (PDF).

AUTHOR INFORMATION

Corresponding Author

*E-mail: paul.dyson@epfl.ch.

ORCID

Paul J. Dyson: 0000-0003-3117-3249

Notes

The authors declare no competing financial interest.

ACKNOWLEDGMENTS

This work was supported by the NCCR Chemical Biology, funded by the Swiss National Science Foundation.

REFERENCES

(1) Finkelstein, J. *Nature* **2009**, *460*, 813−813.
(2) Medici, S.; Peana, M.; Nurchi, V. M.; Lachowicz, J. I.; Crisponi, G.; Zoroddu, M. A. *Coord. Chem. Rev.* **2015**, *284*, 329−350.
(3) Tchounwou, P. B.; Yedjou, C. G.; Patlolla, A. K.; Sutton, D. J. *EXS* **2012**, *101*, 133−164.
(4) Duarte, I. F.; Lamego, I.; Marques, J.; Marques, M. P. M.; Blaise, B. J.; Gil, A. M. *J. Proteome Res.* **2010**, *9*, 5877−5886.
(5) Melnikov, S. V.; Söll, D.; Steitz, T. A.; Polikanov, Y. S. *Nucleic Acids Res.* **2016**, *44*, 4978−4987.
(6) Quintanar, L.; Rivillas-Acevedo, L. *Methods Mol. Biol.* **2013**, *1008*, 267−297.
(7) Murray, B. S.; Menin, L.; Scopelliti, R.; Dyson, P. J. *Chem. Sci.* **2014**, *5*, 2536−2545.
(8) Moreno-Gordaliza, E.; Cañas, B.; Palacios, M. A.; Gómez-Gómez, M. M. *Anal. Chem.* **2009**, *81*, 3507−3516.
(9) Moreno-Gordaliza, E.; Cañas, B.; Palacios, M. A.; Gómez-Gómez, M. M. *Analyst* **2010**, *135*, 1288.
(10) Li, H.; Lin, T.-Y.; Van Orden, S. L.; Zhao, Y.; Barrow, M. P.; Pizarro, A. M.; Qi, Y.; Sadler, P. J.; O'Connor, P. B. *Anal. Chem.* **2011**, *83*, 9507−9515.
(11) Meier, S. M.; Tsybin, Y. O.; Dyson, P. J.; Keppler, B. K.; Hartinger, C. G. *Anal. Bioanal. Chem.* **2012**, *402*, 2655−2662.
(12) Casini, A.; Gabbiani, C.; Michelucci, E.; Pieraccini, G.; Moneti, G.; Dyson, P. J.; Messori, L. *JBIC, J. Biol. Inorg. Chem.* **2009**, *14*, 761−770.
(13) Khalaila, I.; Allardyce, C. S.; Verma, C. S.; Dyson, P. J. *ChemBioChem* **2005**, *6*, 1788−1795.
(14) Erales, J.; Gontero, B.; Whitelegge, J.; Halgand, F. *Biochem. J.* **2009**, *419*, 75−86.
(15) Qi, Y.; Liu, Z.; Li, H.; Sadler, P. J.; O'Connor, P. B. *Rapid Commun. Mass Spectrom.* **2013**, *27*, 2028−2032.
(16) Sze, C. M.; Shi, Z.; Khairallah, G. N.; Feketeová, L.; O'Hair, R. A. J.; Xiao, Z.; Donnelly, P. S.; Wedd, A. G. *Metallomics* **2013**, *5*, 946−954.
(17) Hartinger, C. G.; Groessl, M.; Meier, S. M.; Casini, A.; Dyson, P. J. *Chem. Soc. Rev.* **2013**, *42*, 6186−6199.
(18) Szpunar, J. *Anal. Bioanal. Chem.* **2004**, *378*, 54−56.
(19) Loo, J. A.; A. Benchaar, S.; Zhang, J. *Mass Spectrom.* **2013**, *2*, S0013.
(20) Doerr, A. *Nat. Methods* **2008**, *5*, 24−24.
(21) Hartinger, C. G.; Tsybin, Y. O.; Fuchser, J.; Dyson, P. J. *Inorg. Chem.* **2008**, *47*, 17−19.
(22) Li, H.; Snelling, J. R.; Barrow, M. P.; Scrivens, J. H.; Sadler, P. J.; O'Connor, P. B. *J. Am. Soc. Mass Spectrom.* **2014**, *25*, 1217−1227.
(23) Patiny, L.; Borel, A. *J. Chem. Inf. Model.* **2013**, *53*, 1223−1228.
(24) cheminfo-js/chemcalc-extended, https://github.com/cheminfo-js/chemcalc-extended, accessed December 1, 2016.
(25) Chabner, B. A. *Cancer Res.* **2010**, *70*, 428−429.
(26) Launay-Vacher, V.; Rey, J.-B.; Isnard-Bagnis, C.; Deray, G.; Daouphars, M. *Cancer Chemother. Pharmacol.* **2008**, *61*, 903−909.
(27) Gibson, D.; Costello, C. *Eur. Mass Spectrom.* **1999**, *5*, 501.
(28) Zhao, T.; King, F. L. *JBIC, J. Biol. Inorg. Chem.* **2011**, *16*, 633−639.
(29) Scolaro, C.; Bergamo, A.; Brescacin, L.; Delfino, R.; Cocchietto, M.; Laurenczy, G.; Geldbach, T. J.; Sava, G.; Dyson, P. J. *J. Med. Chem.* **2005**, *48*, 4161−4171.
(30) Konermann, L.; Douglas, D. J. *J. Am. Soc. Mass Spectrom.* **1998**, *9*, 1248−1254.
(31) Davies, M. S.; Berners-Price, S. J.; Hambley, T. W. *Inorg. Chem.* **2000**, *39*, 5603−5613.

DOI: 10.1021/acs.analchem.7b02211
Anal. Chem. 2017, 89, 11985−11989